APS physics

CHORUS

This is the accepted manuscript made available via CHORUS. The article has been published as:

Elastic scattering of low-energy electrons from toluene

Ahmad Sakaamini, L. R. Hargreaves, M. A. Khakoo, D. F. Pastega, and M. H. F. Bettega

Phys. Rev. A **93**, 042704 — Published 11 April 2016

DOI: 10.1103/PhysRevA.93.042704

Elastic Scattering of Low Energy Electrons from Toluene,

Ahmad Sakaamini [1*], L. R. Hargreaves [1], M. A. Khakoo [1], D. F. Pastega [2] and M. H. F. Bettega [2]

[1] Department of Physics, California State University, Fullerton, CA 92831, USA.

[2] Departamento de Física, Universidade Federal do Paraná, Caixa Postal 19044, 81531-990 Curitiba, Paraná, Brazil

* Present Address: The School of Physics and Astronomy, The University of Manchester, Manchester, M13 9PL, United Kingdom

Abstract: Theoretical and normalized experimental differential, momentum transfer and integral cross sections for vibrationally elastic scattering of low-energy electrons from toluene ($C_6H_5CH_3$) are presented. The differential cross sections are measured at incident energies from 1 to 20 eV and scattering angles from 15^o to 130^o. The calculated cross sections are obtained using the Schwinger multichannel method with pseudopotentials in the static-exchange plus polarization approximation. Comparisons are made between the present theory and measurements with earlier available measurements. In general, the agreement between the theory and the experiment is very good. We also discuss the resonance spectra of toluene, where we find three π^* shape resonances whose locations agree well with the experiment. In addition, we compare the cross sections of toluene and benzene, since the former can be considered as a benzene derivative by the substitution of a hydrogen in benzene by a CH_3 group in toluene.

PACS number(s): 34.80.Bm, 34.80.Gs

I. Introduction

Collisions of low-energy electrons with gaseous aromatic polyatomic molecules are of interest in studying variations of aromatics (e.g. furans) found in organic systems such as DNA. The interest in these systems was brought up by the electron attachment work of [1] which concerned breakup of C=C bonds in these compounds by low energy electrons in the form of π^* resonances. The most commonly encountered aromatic compound is benzene. Its usual structural representation is a six-carbon ring (represented by a hexagon) that includes three double bonds alternating between the carbon atoms. The π-bonds in the double bonds delocalize according to the Hückel method and electron attachment to them is of interest, since in electron collisions processes they are responsible for formation of π^* resonances. To each C-atom is also bonded an H-atom via a σ-bond. Replacing one H-atom with a methyl group to form the benzene derivative toluene provides some interesting effects such as the lifting of degeneracy of the two lowest occupied π orbitals in the C-atom thus causing shifts in the energy of the electron attachment negative ion resonances [2, 3] as well as increasing the cross section for electron attachment [4,5].

Presently, there is a paucity of theoretical and experimental effort to investigate resonant electron scattering from simple carbon ring-compounds such as benzene and toluene. In the existing measurements of benzene [11,12], agreement between theory and experiment at low incident electron energies is not satisfactory. Similarly for recent work in toluene [9] there is disagreement between theory and experiment at low energies and consequently a need for experimental and theoretical low energy differential scattering as an important check. In addition, the role of negative-ion resonances regarding differential elastic scattering of electrons from it at low energies still is incomplete. While theory has been satisfactorily tested with other linear polyatomic targets (see e.g. [5a, 23]) it has not been as well in ring compounds, which should be

considered a further step in electron-polyatomic collisions studies. The present work will incorporate theory which will be augmented with experimental work which (unlike conventional experiments) uses a variation of the relative flow method involving a well-tested setup in our laboratory that does not require quantitative information on the gas kinetic molecular diameter of the target and test calibration gases used, and being free of this systematic error, is able to provide reliable, quantitative cross sections for elastic electron scattering from especially large mass ring compound targets such as toluene.

A lower mass ring-compound relative of toluene, benzene has two π^* resonances, the lower being two fold degenerate belonging to the E_{2u} symmetry and located at 1.14 eV, and the higher-lying resonance being a mixture of shape and core excited resonances located at 4.85 eV in the B_{2g} symmetry [6,7]. We expect to observe three resonances in toluene due to the symmetry breaking resulting from the substitution of a H-atom in benzene by a CH_3 group in toluene. The investigation of the resonance spectra of toluene in elastic electron scattering process would probe the effect of this substitution. In addition, this is a start in our theoretical-experimental effort to look at larger ring-type compounds and we aim to next work on xylene isomers [5c].

Past work on electron-toluene ($C_6H_5CH_3$) scattering has been the total cross sections (TCS) of Kato et al. [8] for incident electron energies (E_0) ranging from 0.4 eV to 1000 eV and the differential cross section (DCS) work of Kato et al. [9] for eight values of E_0 ranging from 1.5eV to 200eV and scattering angles (θ) ranging from 15^o to 130^o. They also looked at a fluorinated derivative of benzene, benzotrifluoride ($C_6H_5CF_3$), at the same E_0 and θ values. In both the toluene work of [8] and [9] the cross sections were compared to the experimental benzene TCS work of Makochekanwa et al. [10] and the DCS work of Cho et al. [11] (which includes the data of Gulley and Buckman [12] in it) to determine the effect of the added CH_3 group to the benzene ring

replacing a H atom. In their toluene DCS paper Kato et al. [9] employed the independent-atom method (IAM) corrected using a screen corrected additivity rule (SCAR) which is expected to work at higher E_0 values(typically above 20-30 eV). The DCS angular distributions for electron scattering from toluene [9] and benzene [11] can be expected to be different at small θ, especially at low E_0 since toluene has a small, but significant, non-zero dipole moment of 0.375D [9]. However, the DCSs for benzene and toluene from [9] and [11] were very similar at low E_0 even at small θ. Past work in electron-toluene which examines resonant processes are the threshold electron trap method of Christophorou et al. [2] and electron transmission measurements of Mathur and Hasted [3]. The work of Christophorou et al. [2] found low-lying resonances at 0.4eV, 1.6eV (their range of energy was from ≈0.5eV to 3eV). Mathur and Hasted [3] (with an energy range of just over 1eV to 11eV) observed two low-lying resonances at the energies of 1.27±0.03eV and 4.9±0.1eV, and a broad resonance at 8.18±0.08eV, plus a point of inflexion at between 3 to 3.5eV. These values disagreed with the positions determined in [8]. However, the TCS measurements of Kato et al. [9] show maxima at 1.4eV and 8 eV with a point of inflexion at 4.5eV, more in agreement with the results of [3]. The elastic integral cross sections (ICS) of Kato et al. [9], determined from their elastic differential cross sections, show good agreement with the TCSs (about 10-15% below the TCSs at below the ionization potential, which is approximately of the magnitude to allow for inelastic processes such as vibrational and electronic excitation) of [8] except at their lowest energy of 1.5eV where their ICSs are considerably lower (<70%) than their TCSs.

In the present work, we present integral, differential and momentum transfer cross sections for elastic scattering from toluene as part of an effort to study benzene derivatives with substituting a $–CH_3$ group on one of the –H groups. We have also planned similar work on substituting two –

CH_3 groups to produce o-xylene, m-xylene and p-xylene [13]. For all these targets we have conducted a joint experimental and theoretical study to provide low energy differential elastic and integral cross sections, and to compare our results with theory and other available (experimental) cross sections. To calculate the cross sections we employed the Schwinger multichannel method with pseudopotentials, in the static-exchange plus polarization approximation.

The remainder of this paper is as follows. In Sec. II we describe the experimental and theoretical methods used. In Sec. III we make our comparisons and inferences and in Sec. IV we finalize with our overall conclusions. In this work our DCSs were taken at E_0 values of 1.00eV, 1.50eV, 2.00eV, 3.00eV, 5.00eV, 8.50eV, 10.0eV, 15.0eV and 20.0eV and θ from 15^o to 130^o.

IIa. Experimental

Our experimental setup has been detailed previously, e.g. Khakoo et al. [14], and so only a brief description will be given here. Both the electron gun and detector employed double hemispherical energy selectors, and the apparatus was made of titanium. Cylindrical lenses were used to transport scattered electrons through the system which was baked to about 130^o with magnetically free biaxial heaters [15]. Electrons were detected by a discrete dynode electron multiplier [16] with a dark count rate of <0.01Hz and capable of linearly detecting $>10^5$ Hz without saturating. The remnant magnetic field in the collision region area was reduced to ≈1mG at the collision region by a double μ-metal shield, coupled with a Helmholtz coil that eliminated the vertical component of the Earth's magnetic field. Typical electron currents were around 18-25 nA, with an energy resolution of between 40-70meV, full-width at half-maximum. Lower currents were chosen for lower E_0 values in order to curtail the effects of space charge broadening of the incident electron beam. The electron beam could be easily focused at 1 eV and remained stable, varying less than 15% at maximum during the day's data acquisition. The energy of the beam was

established by repetitively (at least daily) measuring the dip in the elastic scattering of the 2^2S He-resonance at 19.366eV [17] at $\theta=90^o$ to better than ≈40meV stability during an experimental run (1 day).

Typically the contact potential varied from 0.6 eV to 0.7 eV. Energy loss spectra of the elastic peak were collected at fixed E_0 values and θ by repetitive, multi-channel-scaling techniques. The effusive target gas beam was formed by flowing gas through a 0.3mm diameter aperture, which was sooted (using an acetylene flame) to reduce secondary electrons. In using the aperture instead of a conventional tube gas collimator, we obviate the experimental need to maintain the gas pressures of the target gases in an inverse ratio of their molecular diameters, thus removing an additional systematic source of error that could occur in using tube collimators or similar, see e.g. [18]. The aperture, located ≈7mm below the axis of the electron beam, was incorporated into a moveable source [18, 19] arrangement. The moveable gas source method determines background electron-gas scattering rates expediently and accurately [19]. The measured DCSs were normalized using the Relative Flow Method with helium as the reference gas, using DCSs from the well-established work of Nesbet [20] for E_0 below 20eV and of Register et al. [21] for E_0 above 20eV. The pressures behind the aperture ranged from 1.2 to 2 torr for He and 0.08 to 0.11 torr for toluene, resulting in a chamber pressure ranging from $1.0x10^{-6}$ torr to $2x10^{-6}$ torr. Toluene has a high molecular mass (92.14 a.m.u.) and is the heaviest target so far used in our system. It was found to be significantly viscous and caused instabilities in the flow as it blocked our high quality gas bleed valve (Granville-Phillips Series 203 valve, [22]). In this case we also baked the valve at its inlet (where the blockage was occurring) to a temperature of about 60-70^{o}C. Also, the entire gas line after the bleed valves was heated to ≈84^{o}C to prevent condensation of toluene. This procedure took care of the valve blockages and stabilized our flow rate to better than 10% during our toluene runs.

Each DCS was taken a minimum of two times to check its reproducibility and weighted averaging was made of multiple data sets to obtain the final DCSs. Integral cross sections (ICS) and Momentum Transfer Cross Sections (MTCS) were evaluated from the measured DCS by extrapolating the DCS to $\theta=0^o$ and 180^o as described in [23] and numerically integrating the extrapolations using a spline fit.

IIb. Theoretical

To compute the elastic integral, differential and momentum transfer cross sections of toluene, we employed the well-established Schwinger multichannel method (SMC) [24], implemented with norm-conserving pseudopotentials (SMCPP) [25]. The SMC method and its implementations are described in detail elsewhere [26]. Therefore, we will only discuss the theoretical aspects of the method that are related to the present calculations.

Our calculations were carried out at the ground state geometry of toluene (represented in Figure 1), which belongs to the C_s symmetry group. In order to optimize the toluene ground state geometry, we employed the density functional theory (DFT) with B3LYP functional and the aug-cc-pVDZ basis set, as implemented in the package GAMESS [27]. In the scattering calculations we used the norm-conserving pseudopotentials of Bachelet *et al.* [28] in order to replace the core electrons of the carbon atoms, and the valence electrons are represented by six *s*-type, five *p*-type and one *d*-type Cartesian Gaussian functions, generated according [29]. For the hydrogens we employed the 4s/3s basis set of Dunning [30] augmented with one p-type function with an exponent 0.75. The symmetric combinations of the *d*-type orbital were excluded to avoid linear dependency in the basis set. With this level of calculation we also obtained a dipole moment of 0.381 D, just 1.6 % greater than the experimental value in [9].

In this work we present our calculations in the static-exchange plus polarization (SEP) approximation, where the configuration-state functions (CSFs) are built from products of target states with single-particle functions. In the static-exchange (SE) approximation, where target polarization is completely neglected,the CSFs are given by a direct product between the target ground state and a single-particle function. In the SEP approximation, the SE basis space is augmented by including CSFs built as a direct product between N-electron states obtained by performing single excitations of the target from the occupied (hole) orbitals to a set of unoccupied (particle) orbitals, and a single-particle function. We employed modified virtual orbitals (MVO) [31] to represent the particle and the scattering orbitals. These orbitals were generated by diagonalizing a cationic Fock operator with charge +6. The SEP space was formed by singlet (SEP(s)) and singlet+triplet-coupled (SEP(s+t)) excitations from all valence orbitals to the 50 lowest MVOs. We obtained 20516 (10406 in A' and 10110 in A'' symmetries) CSFs in the SEP(s) calculations and 19914 (10025 in A' and 9789 in A'' symmetries) CSFs in SEP(s+t) calculations. Lastly we employed the standard Born-closure procedure [32] to account for scattering of the higher partial waves, due the long –range character of the dipole potential of the molecule

III. Results and Discussion.

Our experimental DCSs are listed in Table 1 along with standard deviation errors determined from statistics of the background subtracted scattered electron counts, reproducibility of the DCSs, and estimated errors in gas flow-rates (2% for He and 3% for toluene) and in the helium elastic DCSs (5 to 7%) used for normalization of the toluene DCSs.

Our experimental and calculated DCSs are shown in figure 2 along with the DCSs for benzene measured by Cho et al. [11]. At our lowest E_0 of 1eV, a comparison of the present DCSs with

those of benzene from Cho et al. [11] shows a major difference between the two targets. Whereas the benzene DCSs is entirely backward peaking, that of toluene shows clear forward peaking. This behavior is very likely on account of differences in their dipole moments. The dipole polarizabilities of these molecules have similar values of 123.1Å^3 and 103.3 Å^3 [33,34] for toluene and benzene, respectively. Benzene has no permanent dipole moment and so very likely the permanent dipole of toluene affects its forward scattering behavior in this case. Unfortunately, we are unable to measure DCSs at $\theta<25^o$ to test theoretical models at smaller θ. This is because of increased forward scattering electron backgrounds, due to the forward electron beam, which swamp our scattered electron signal at these small θ. However, we still observe an earlier rise in the DCSs which is not observed in the Born-corrected SMC models. At E_0 of 1.5eV, we can compare with DCSs of Kato et al. [9] and find significant differences between them for $\theta<70^o$. At E_0=1eV and 1.5eV the present experimental data agree well with the SMC SEP(s) with Born closure for angles above 50^o. We can now compare again the DCSs of toluene and benzene at E_0=2eV and 3eV, where the benzene DCSs show significant differences at small θ, as expected due to the permanent electric dipole moment of toluene., while at 3eV the DCSs agree quite well at high scattering angles. For impact energies above 3eV, the agreement between the experimental DCSs is very good with small differences at small θ. The present computed DCSs are also in good agreement with the experiment until E_0=10eV, while at higher energies the computed DCSs lies above the experiment. This behavior is expected since in our calculations we are considering only the elastic channel as an open channel. The effect of multichannel coupling on the elastic channel is to lower the cross sections, since there is flux loss from the elastic to the inelastic channels [35-37]. At these energies above 5eV the benzene elastic DCSs of Cho et al. [11] are found to be the

same at $\theta<30^{o}$, but lower at larger θ by about 30-40% on average, although shape-wise both large θ DCSs are essentially flat.

Figure 3 show the ICSs and MTCSs for toluene. Our ICSs are in very good agreement with the TCSs of Kato et al. [8] , being about 10-20% lower at below the ionization potential of toluene, which is typical of electronic and vibrational excitation below the ionization potential. The DCS of Kato et al. [9] also shows very good agreement with ours except at E_0=1.5eV where it is lower by a factor of 80%. The biggest differences between the present experimental data and the calculations are found in energies below 3 eV due to the presence of the shape resonances. In the SEP(s) calculations the two low-lying resonances are located at 1.8 and 2.1eV respectively, while in the SEP(s+t) calculations the same resonances are located at 0.7 and 1.0 eV. Our experimental MTCS are in very good agreement with Kato's at all energies. Calculated MTCS only disagree with the experimental data for energies greater than 10 eV. This is primarily due to the fact that differences in forward scattering in the DCSs do not contribute as much to the MTCSs as it does to the ICSs, due to the additional (1 - cos θ) weighting factor in the former.

In Fig. 4 we observe a sharp maximum typical of a π^* resonance at E_0=1.5±0.07eV, which is however observed in the SMC models at lower energy. As shown in figure 3, our calculations show the presence of three π^* resonances. In the SEP(s+t) calculations, the first resonance is located at 0.7 eV, the second at 1 eV and the third at 5.5 eV. Christophorou [2], reported the two low-lying resonances at 0.4 and 1.6, while Mathur et al. [3] reported the second π^* resonance at 1.27 eV, and the third at 4.9 eV. Therefore our calculations are in reasonable agreement with the previous experimental reports of the resonances and also with the present experimental data. It is worth to mention that the higher-lying resonance is a mixture of a shape and core excited resonances, and belongs to the same symmetry of the second resonance. This poses an additional

difficulty in dealing with these resonances, since in order to obtain a better description of the location of the third resonance requires singlet and triplet coupling in the description of polarization effects [7], which may overcorrelate the low-lying resonance, placing it below the experimental position. Agreement with the $\theta=90^o$ DCSs of Kato et al. [9] is excellent except at E_0=1.5eV similar to the case of the ICSs at this E_0 value in Fig. 3.

As mentioned before, the substitution of a hydrogen atom in benzene by a methyl group in toluene breaks the symmetry and removes the degeneracy of the lowest occupied π* orbital of toluene. In Figure 5 we present the symmetry decomposition of the ICS into partial cross sections (CS) for each irreducible representation of the C_s symmetry group, namely *A'* and *A''*, along with the corresponding unoccupied molecular orbitals. These orbitals were obtained in a bound state calculation with a small basis set using GAMESS, and in a simple model (based on the Koopmans theorem) could be viewed as the orbitals responsible for the resonances . From this figure it is possible to observe that the two low-lying π* resonances of toluene are no longer degenerate, since they are located at different (although close) energies and belong to different representations of the C_s group. Inaddition, the low-lying resonance of toluene stabilizes with respect to the low-lying resonance of benzene.

IV. Conclusions.

We have presented low energy theory and measurements of DCSs for vibrationally elastic electron scattering from toluene. Agreement between theory and experiment is in most cases very good, except at energies below 2eV, where significant differences are found. We experimentally located the position of the π* resonance at 1.5eV, but this is not precisely determined in the theory, i.e. at 1eV or at 2eV depending on which channels (singlet and triplet or both) are included. Comparison with benzene shows expected differences at small scattering angles at very low energy

and at large scattering angles at energies of 5eV and greater. This work is an effort to explore electron scattering from benzene derivatives, which will be followed by similar work on the o-, m-, and p- xylenes isomers.

V. Acknowledgements.

M. A. K. and L. R. H. acknowledge support from National Science Foundation Research in an Undergraduate Institution grants NSF-RUI-AMO 1306742 and 0968874. D. F. P. acknowledges support from Brazilian Agency Coordenação de Aperfeiçoamento de Pessoal de Nível Superior (CAPES). M.H.F.B. acknowledges support from Brazilian agencies Conselho Nacional de Desenvolvimento Científico e Tecnológico (CNPq), and Financiadora de Estudos e Projetos (FINEP), under project CTInfra. D. F. P. and M.H.F.B also acknowledge computational support from Professor Carlos M. de Carvalho at LFTC-DFis-UFPR and at LCPAD-UFPR, and from CENAPAD-SP.

VI. References.

[1] B. Boudaïffa, P. Cloutier, D. Hunting, M. A. Huels and L. Sanche, Science, **287**, 1658 (2000).

[2] L. G. Christophorou, D. L. McCorkle and J. G. Garner, J. Chem. Phys. **60**, 3779 (1974).

[3] D. Mathur and J. B. Hasted, J. Phys. B: At. Mol. Phys. **9**, L31 (1976).

[4] S. L. Lunt, D. Field, S. V. Hoffmann, R. J. Gulley, and J-P. Ziesel, J. Phys. B **32**, 2707 (1999).

[5] J. K. Olthoff, J. A. Tossell, and J. H. Moore, J. Chem. Phys. **83**, 5627 (1985).

[5a] A. Gauf, L. R. Hargreaves, A. Jo, J. Tanner, M. A. Khakoo, T. Walls*, C. Winstead and V. Mckoy, Phys. Rev A. 85, 052717 (2012).

[6] I. Nenner and G. J. Schulz, J. Chem. Phys. **62**, (1975).

[7] C. Winstead and V. McKoy, Phys. Rev. Lett. **98** (2007).

[8] H. Kato, C. Makochekanwa, Y. Shiroyama, M. Hoshino, N. Shinohara, O. Sueoka, M. Kimura, and H. Tanaka, Phys. Rev. A **75**, 062705 (2007).

[9] H. Kato, M. C. Garcia, T. Asahina, M. Hoshino, C. Makochekanwa and H. Tanaka, Phys. Rev. A **79**, 062703 (2009).

[10] C. Makochekanwa, O. Sueoka, and M. Kimura, Phys. Rev. A 68, 032707 (2003).

[11] H. Cho, R. J. Gulley, K. Sunohara, M. Kitajima, L. J. Uhlmann, H. Tanaka, and S. J. Buckman, J. Phys. B **34**, 1019 (2001).

[12] R. J. Gulley and S. J. Buckman, J. Phys. B **32**, L405 (1999).

[13] A. Sakaamini, S. M. Khakoo, L. R. Hargreaves, M. A. Khakoo, D. F. Pastega and M. H. F. Bettega, Phys. Rev. A., In Progress. To be submitted to Phys. Rev. A.

[14] M. A. Khakoo, C. E. Beckmann, S. Trajmar and G. Csanak, Phys. Rev. A **27**, 3159 (1994).

[15] ARi Industries Inc., Addison, IL 60101 USA, 1HN040B-16.3 biaxial cable.

[16] ETP Equipe Thermodynamique et Plasmas (ETP) model AF151.

[17] J. H. Brunt, G. C. King, and F. H. Read, J. Phys. B: At. Mol. Phys. **10**, 1289 (1977).

[18] M. A. Khakoo, K. Keane, C. Campbell, N. Guzman and K. Hazlett, J. Phys. B. **40**, 3601 (2007)

[19] M. Hughes, K. E. James, Jr., J. G. Childers, and M. A. Khakoo, Meas. Sci. Technol. **14**, 841 (1994).

[20] R. K. Nesbet, Phys. Rev. A **20**, 58 (1979).

[21] D. F. Register, S.Trajmar, and S. K. Srivastava, Phys. Rev. A **21**, 1134 (1980).

[22] MKS, Granville-Phillips Division, 6450 Dry Creek Parkway, Longmont, CO 80503 USA.

[23] K. Fedus, C. Navarro, L. R. Hargreaves, and M. A. Khakoo, F. M. Silva and M. H. F. Bettega, C. Winstead and V. McKoy, Phys. Rev. A **90**, 032708 (2014).

[24] K. Takatsuka and V. McKoy, *Phys. Rev. A* **24**, 2473 (1981); *Phys. Rev. A* **30**, 1734 (1984).

[25] M. H. F. Bettega, L. G. Ferreira, and M. A. P. Lima, *Phys. Rev. A* **47**, 1111 (1993).

[26] R. F. da Costa, M. T do N. Varella, M. H. F. Bettega, and M. A. P. Lima, *Eur. Phys. J. D* **69**, 159 (2015).

[27] M.W. Schmidt, K. K. Baldridge, J. A. Boatz, S. T. Elbert, M. S. Gordon, J. H. Jensen, S. Koseki, N. Matsunaga, K. A. Nguyen, S. J. Su, T. L. Windus, M. Dupuis, and J. A. Montgomery, *J. Comput. Chem*. **14**, 1347 (1993).

[28] G. B. Bachelet, D. R. Hamann, and M. Schlüter, *Phys. Rev. B* **26**, 4199 (1982).

[29] M. H. F. Bettega, A. P. P. Natalense, M. A. P. Lima, and L. G. Ferreira, *Int. J. Quantum Chem*. **60**, 821 (1996).

[30] T. H. Dunning, Jr., *J. Chem. Phys*. **53**, 2823 (1970).

[31] C. W. Bauschlicher, Jr., J. Chem. Phys. **72**, 880 (1980).

[32] E. M. de Oliveira, M. T. do N. Varella, M. H. F. Bettega, and M. A. P. Lima, *Eur. Phys. J. D* **68**, 65 (2014).

[33] N. K. Sanyal, P. Ahmad, and L. Dixit, J. Phys. Chem. **77**, 7973 (1973).

[34] http://openmopac.net/Polarizability_table.html.

[35] R. F. da Costa, M. H. F. Bettega, M. A. P. Lima, M. C. A. Lopes, L. R. Hargreaves, G. Serna, and M. A. Khakoo, Phys. Rev. A **85**, 062706 (2012).

[36] R. F. da Costa, M. H. F. Bettega, M. T. do N. Varella, E. M. de Oliveira, and M. A. P. Lima, Phys. Rev. A. **90**, 052707 (2014).

[37]R. F. da Costa, E. M. de Oliveira, M. H. F. Bettega, M. T. do N. Varella, D. B. Jones, M. Brunger, F. Blanco, R. Colmenares, P. Limão-Vieira, G. Garcia, and M. A. P. Lima, J. Chem. Phys. **142**, 104304 (2015).

Energy (eV)→								DCS (10^{-16}cm^2/sr)										
Angle (^{o})↓	1.00	Error	1.50	Error	2.00	Error	3.00	Error	5.00	Error	8.50	Error	10.00	Error	15.00	Error	20.00	Error
15											47.1	6.4	34.3	4.7	52.6	6.5	44.1	5.9
20			11.0	1.6	6.78	0.99	7.79	1.07	17.4	2.2	31.2	3.7	23.9	2.7	30.7	3.7	20.4	2.5
25	5.65	1.20	7.61	1.19	5.32	0.60	7.18	0.91	13.1	1.7	18.9	2.0	17.6	2.0	17.5	2.0	9.6	1.1
30	3.92	0.66	4.89	0.68	4.61	0.55	6.42	0.77	10.2	1.6	12.4	1.4	12.4	1.6	9.5	1.1	5.07	0.57
40	2.75	0.37	3.98	0.47	3.93	0.56	5.85	0.74	6.97	1.06	6.12	0.75	5.37	0.69	3.69	0.45	1.99	0.24
50	2.44	0.32	3.55	0.40	3.91	0.60	5.14	0.65	5.52	0.63	3.67	0.42	3.17	0.39	1.98	0.23	1.22	0.14
60	2.42	0.26	3.34	0.38	3.69	0.53	4.48	0.58	3.53	0.45	2.42	0.28	2.62	0.30	1.51	0.19	1.14	0.13
70	2.52	0.32	3.32	0.42	3.92	0.44	3.39	0.41	2.52	0.36	2.30	0.27	2.49	0.29	1.57	0.19	1.00	0.12
80	2.39	0.30	2.98	0.37	2.97	0.33	2.38	0.30	2.27	0.29	2.36	0.29	2.35	0.28	1.35	0.17	0.87	0.11
90	2.15	0.27	2.61	0.34	2.26	0.27	1.58	0.20	2.22	0.31	2.29	0.27	2.30	0.26	1.31	0.16	0.93	0.11
100	2.07	0.31	2.12	0.23	1.80	0.21	1.22	0.14	2.09	0.27	2.16	0.26	2.10	0.25	1.14	0.14	0.75	0.09
110	1.92	0.31	2.22	0.27	1.57	0.22	1.23	0.15	1.94	0.24	2.18	0.26	1.68	0.20	1.10	0.15	0.79	0.10
120	1.79	0.28	2.12	0.29	1.26	0.19	1.17	0.15	1.76	0.22	2.04	0.24	1.35	0.16	1.30	0.17	0.931	0.114
125			1.86	0.29			1.16	0.15	2.04	0.30	1.74	0.21	1.24	0.15	1.41	0.18	0.987	0.112
130							1.16	0.15	2.125	0.337	1.84	0.22	1.29	0.14	1.58	0.20	1.059	0.130
ICS	38.0	7.2	48.8	6.2	43.3	5.8	44.6	5.5	52.0	14.0	72.7	9.2	62.3	8.8	63.7	10.5	54.5	10.1
MTCS	29.5	4.5	33.8	6.5	28.7	4.6	25.8	4.7	31.5	6.7	33.0	4.5	28.2	4.9	24.5	5.7	18.2	6.3

Table 1: Present experimental DCSs plus associated error bars for vibrationally elastic scattering of electrons from toluene. ICSs and MTCSs with error bars are given in the bottom two rows.

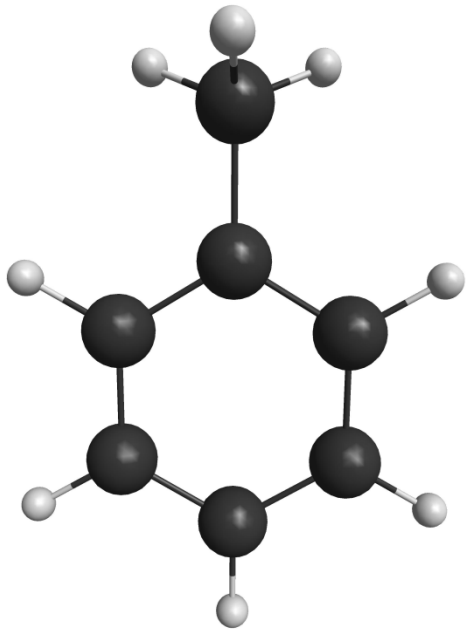

Figure 1: Ball and stick model of toluene. C-atoms are shown in black and h-atoms in white.

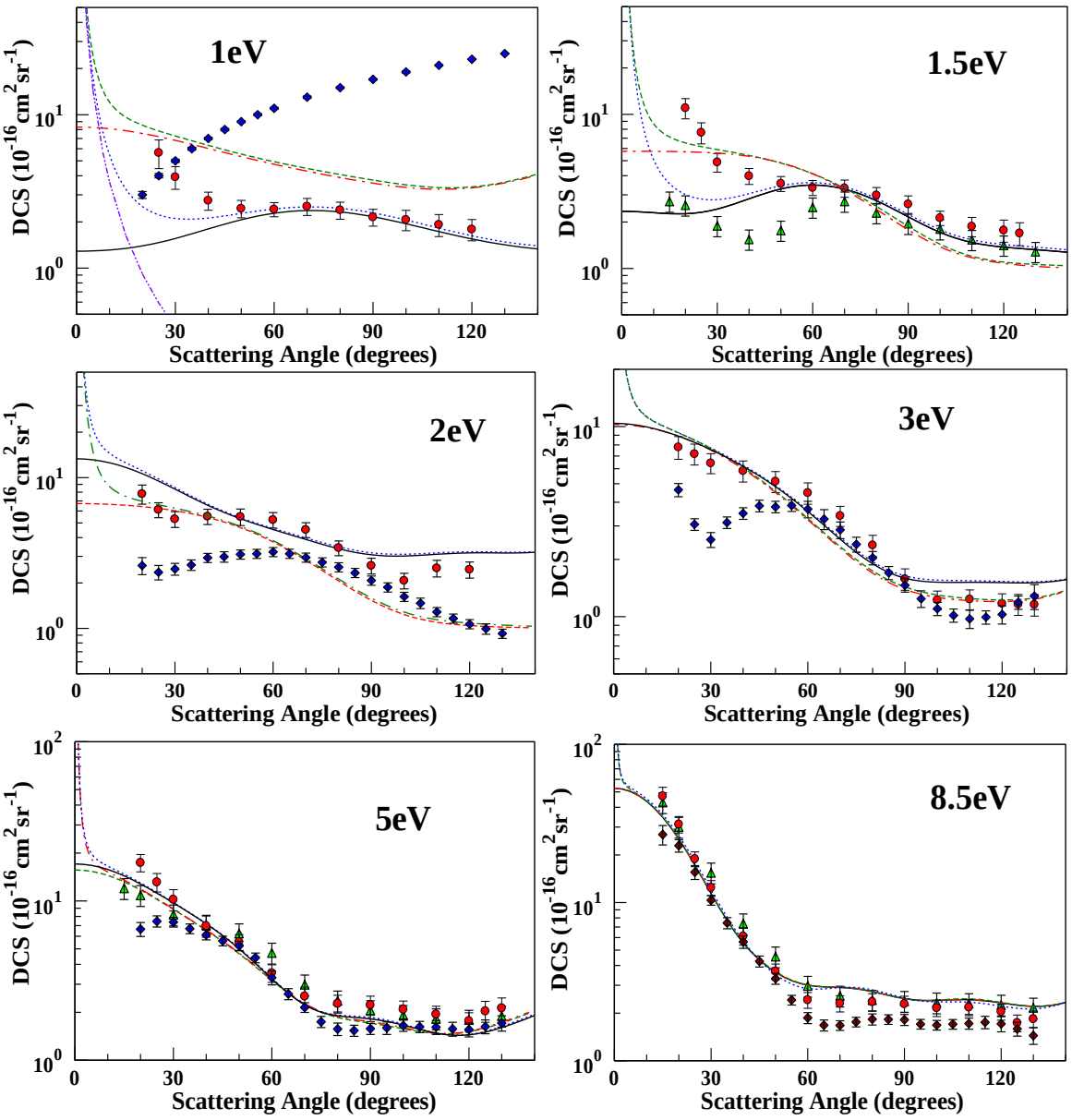
1eV
1.5eV
2eV
3eV
5eV
8.5eV
DCS (10^{-16} cm^{2}sr^{-1})
Scattering Angle (degrees)
0
30
60
90
120
10^0
10^1
10^2

Fig. 2 (part).

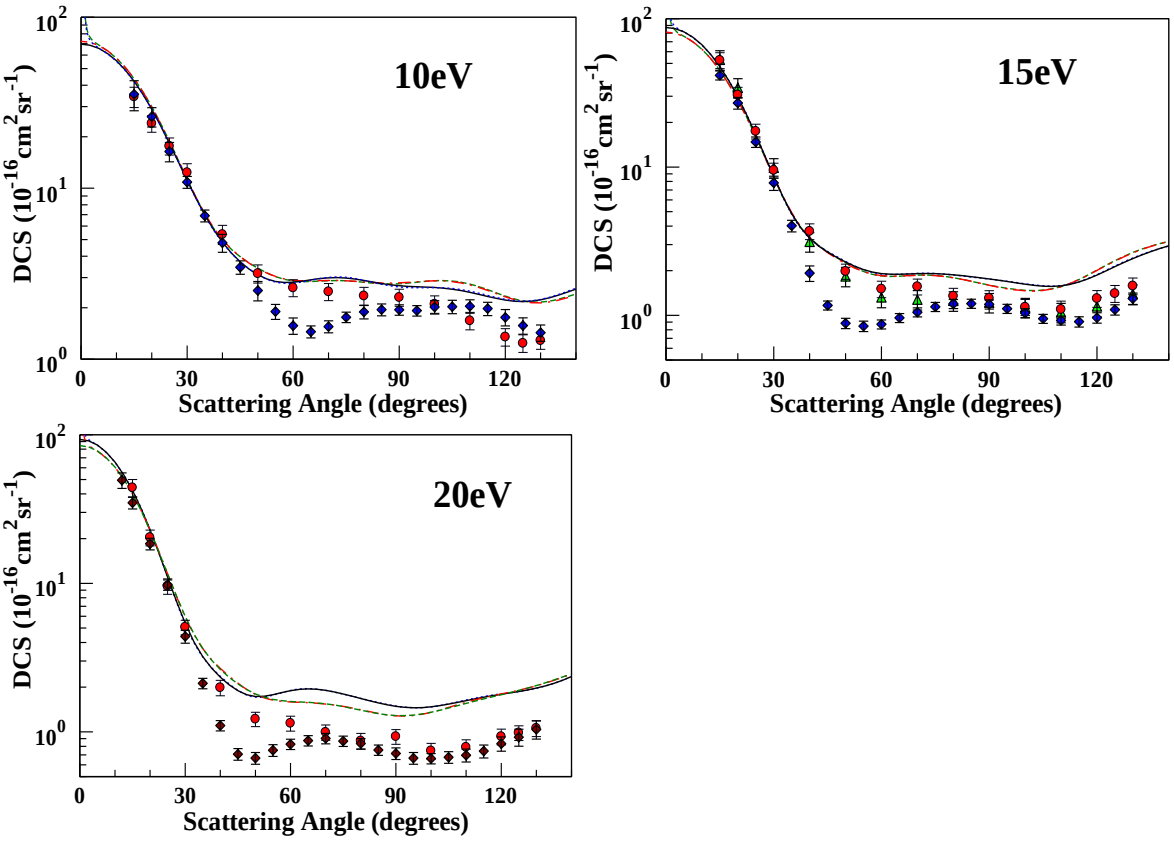

Figure 2 (Color Online): DCSs for elastic scattering of low energy electrons from toluene. Present work: ● present experimental DCSs; SMC theory: —— static-exchange with polarization, singlet coupling only; ---- static-exchange with polarization, singlet coupling only and Born closure; – - – static-exchange with polarization, singlet and triplet coupling and Born closure; – – static-exchange with polarization, singlet and triplet coupling, – - – Born-dipole. Experimental DCSs: ▲ Kato et al. [9]. Experimental benzene DCSs: ♦ Cho et al [11] at the energies of 1.1eV, 2eV, 3eV, 5eV, 10eV, 15eV; ♦ Gulley and Buckman [12] at 20eV.

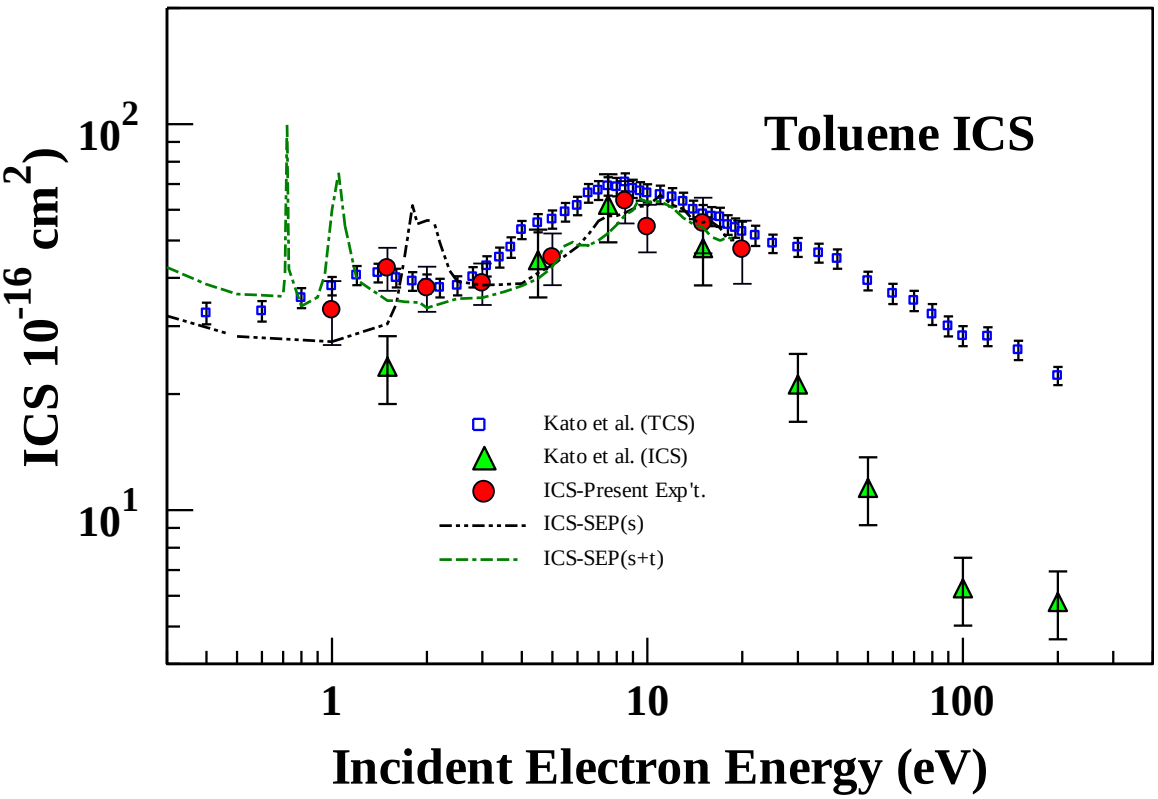

Figure 3a (Color Online): ICSs for elastic scattering of low energy electrons from toluene. Present work: ● present experimental ICS, ▲ Kato et al. [9] ; SMC theory: —··— static-exchange with polarization, singlet coupling only and Born closure; – · – static-exchange with polarization, singlet and triplet coupling and Born closure. Experimental TCSs: □ Kato et al. [8] .

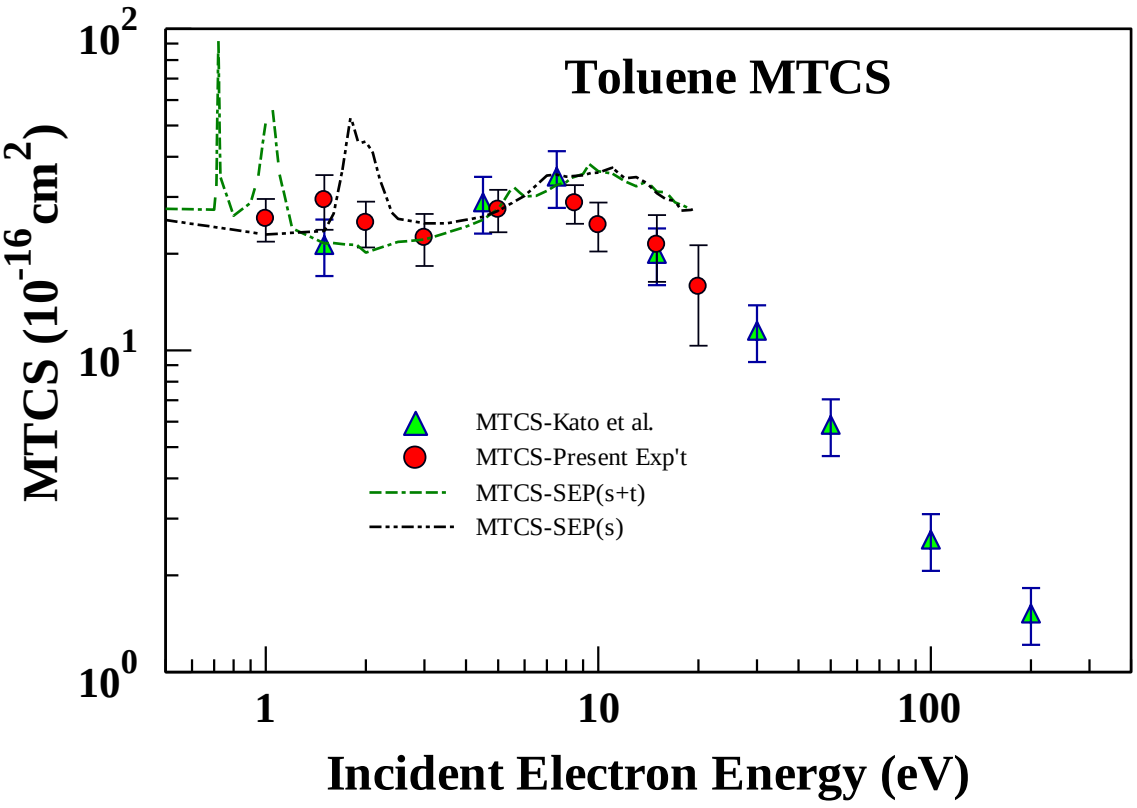

Figure 3b (Color Online): MTCSs for elastic scattering of low energy electrons from toluene. Legend is the same as Fig. 3a.

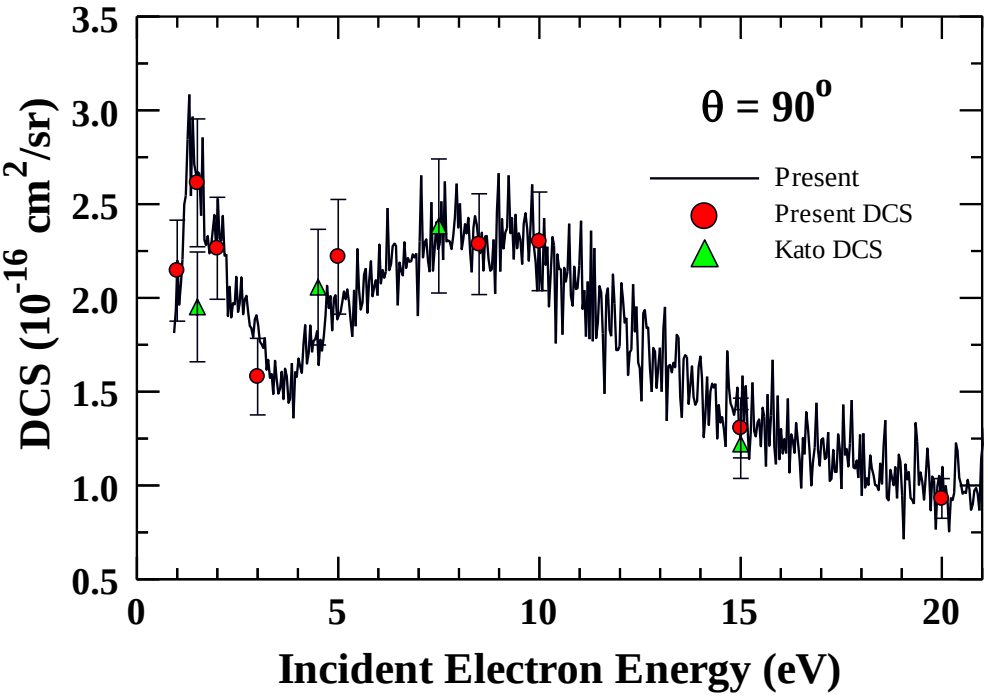

Figure 4 (Color Online): DCSs for elastic scattering of low energy electrons from toluene at θ=90°. Present work: ● present experimental DCSs from Table 1, ▲ Kato et al. DCSs [9] and — θ=90° experimental excitation function.

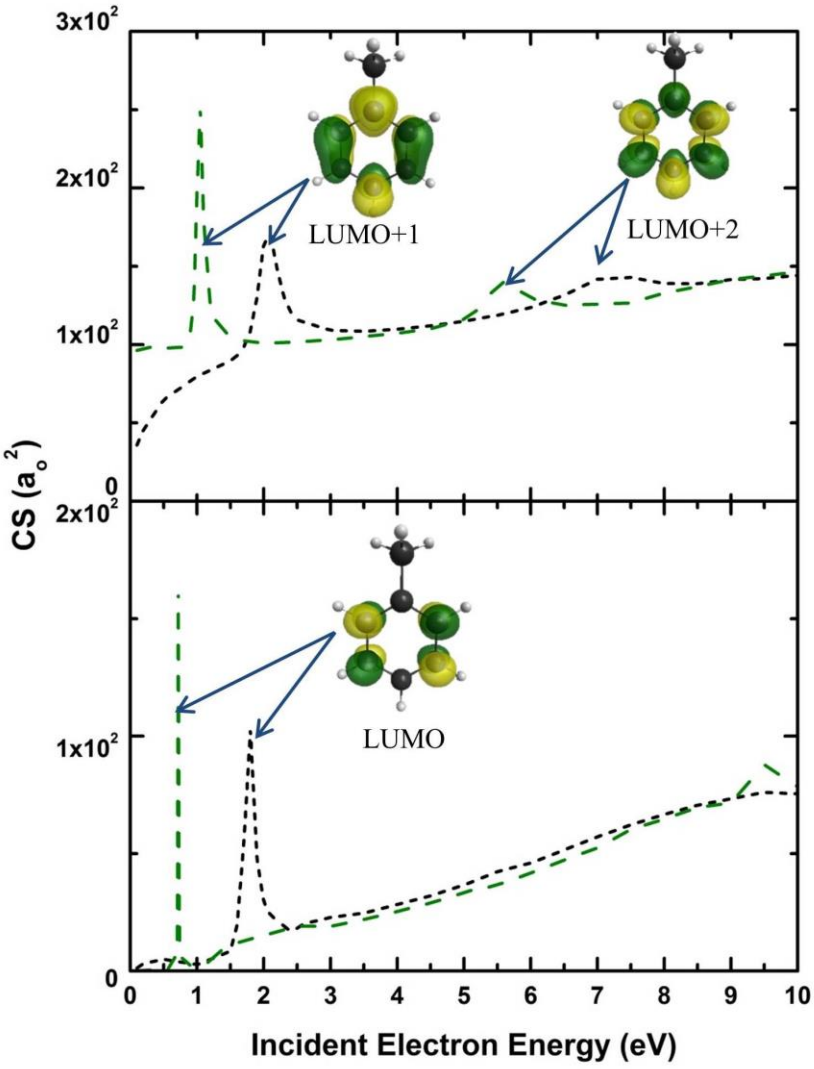

Figure 5 (Color Online): Calculated symmetry decomposition of the ICS into partial cross sections (CS) for each irreducible representation of the C_s . SEP(s) approximation ---- **;** SEP(s+t) approximation – – **.** In the upper panel we show the A' symmetry and in the lower panel we show the A'' symmetry. The different colors mean different orbital signs. See text for discussion.